Upper Bounds on the Heat Transport in Infinite Prandtl Number Convection

S. C. Plasting
University of Bristol, U.K.

Abstract

We study the asymptotic scaling with Rayleigh number, Ra, of the vertical heat transport through a layer of fluid of infinite Prandtl number confined between two horizontal plates. The plates are at fixed temperature with heating from below. Previous work based on Howard's optimum theory yields an upper bound on the Nusselt number, Nu, that scales as $Ra^{1/3}$. Using the Background method a rigorous upper bound of $Ra^{2/5}$ has been deduced and with additional information derived from the governing equations an improved bound of the form $Ra^{1/3}(\log Ra)^{2/3}$ can be derived. In this report we investigate why the Background method falls short of the earlier result obtained using Howard's optimum theory. We show that these two methods seek to optimise the same functional within a min-max scheme. We compute the optimal piecewise linear solution to the Background method and examine the associated eigenfunctions.

1 Introduction

The theoretical study of variational bounds on turbulent transport quantities began in 1963 with Howard's Optimum Theory [1]. In the absence of an incompressibility constraint Howard solved Euler-Lagrange equations analytically to obtain an upper bound on the heat transport in turbulent Boussinesq convection which scaled like $Ra^{1/2}$. Later the constraint of incompressibility was utilised and boundary layer methods were developed to solve Howard's Euler-Lagrange equations for the maximum heat transport problem. Two theoretical tools emerged. The first was the single-α [2], or single horizontal wave-number, test function method. The solutions to the boundary layer equations in this analysis yield a lower bound on the true optimal solution. The second method, due to Busse [3], was the multi-α solutions, a multiple boundary layer solution of the underlying Euler-Lagrange equations, with an arbitrary number of horizontal wave-numbers. Busse's multi-α solution was indeed the optimal solution to Howard's variational problem.

The multi-α solutions of Busse were later used by Chan [4] to calculate an upper bound on the heat transport for the closely related problem of infinite Prandtl number convection. Chan found an improvement to the asymptotic scaling of the upper bound on the heat transport by imposing the momentum equation directly as a point-wise constraint. He calculated an upper bound on the heat transport with an asymptotic scaling of $Ra^{1/3}$.

In the nineties a complementary variational problem for bounding the heat transport in turbulent convection was developed by Doering and Constatin [5]. The so-called Background method seeks to estimate the optimal solution to the maximisation problem from above, therefore any test function satisfying certain well-defined constraints will yield a rigorous upper bound on the heat transport. The duality of the Optimum Theory and the Background method was proved for the problem of arbitrary Prandtl number convection by Kerswell [6]. The Background method has recently been applied to the problem of infinite Prandtl number convection in two distinct ways. First, using piecewise linear test functions and standard functional inequalities an upper bound of $Ra^{2/5}$ was calculated which is uniform in rotation rate for rotation perpendicular to the fluid layer [7]. Second, using the Background method and the extra information that the temperature at any point may not exceed the maximum temperature on the boundary an upper bound of $Ra^{1/3}(\log Ra)^{2/3}$ was deduced [8]. Though not uniform with respect to rotation this upper bound captures the form of Chan's result with a logarithmic correction.

In a number of other fluid problems, namely plane Couette flow, pipe flow or Poisuille flow, and arbitrary Prandtl number convection, piecewise linear test profiles for the Background method have been able to achieve optimal scaling in these variational problems. Since Chan's result implies that the optimal scaling for infinite Prandtl number convection is $Ra^{1/3}$, it is interesting to ask why piecewise linear test profiles do not capture the optimal scaling in this problem. Otero [9] also found a 2/5 scaling by numerically optimising the upper bound over piecewise linear test profiles and hence showed that the functional estimates used to calculate the upper bound in [7] are tight.

The structure of this report is as follows. We first introduce the basic equations for infinite Prandtl number Boussinesq convection and define quantities and derive identities which will be frequently referred to in the rest of our presentation. Secondly we will study the seemingly disparate variational methods of Doering-Otero and of Howard-Chan. We will show that both of these methods can be derived from a single specified functional. We will verify the numerical calculation of the optimal piecewise linear test profiles due to Otero and produce trial functions for Chan's dual problem which will be used to construct lower bounds on the optimal upper bound.

2 Basic Equation and Derived Quantities

We consider convection between two infinitely extended parallel plates with fixed temperature on the plates. We impose no-slip boundary conditions on the plates and periodic boundary conditions for all variables in the $x, y-$plane. Gravity is perpendicular to the impenetrable plates and the fluid sandwiched between the plates is incompressible.

2.1 Basic equations

The basic first order equations of motion for this system are the Rayleigh-Bénard equations. In non-dimensionalised form these are as follows

$$\frac{1}{\sigma}\left(\frac{\partial \mathbf{u}}{\partial t} + \mathbf{u}\cdot\boldsymbol{\nabla}\mathbf{u}\right) + \boldsymbol{\nabla} p = \mathrm{Ra} T\hat{\mathbf{z}} + \Delta\mathbf{u} \tag{1}$$

$$\frac{\partial T}{\partial t} + \mathbf{u}\cdot\boldsymbol{\nabla} T = \Delta T \tag{2}$$

where the control parameters are the non-dimensionalised temperature difference across the layer Ra, the Rayleigh number, and the ratio of kinematic viscosity to thermal diffusivity σ, the Prandtl number. In the limit of infinite Prandtl number the inertial terms in the momentum equation drop and we are left with a linear dependence of the velocity field on temperature

$$\Delta\mathbf{u} + \mathrm{Ra} T\hat{\mathbf{z}} = \boldsymbol{\nabla} p. \tag{3}$$

We can dispense of the incompressibility constraint $\nabla \cdot \mathbf{u} = 0$ and the pressure in the following manner. Let $\mathcal{N} := \Delta \mathbf{u} + \mathrm{Ra} T \hat{\mathbf{z}} - \nabla p = 0$ and denote by $\mathcal{N}_3$ the third component of $\mathcal{N}$. The components of Equation (3) are

$$\begin{aligned} \Delta u &= p_x \\ \Delta v &= p_y \\ \Delta w + \mathrm{Ra} T &= p_z \end{aligned}$$

where $\mathbf{u} = (u, v, w)$. With the help of incompressibility taking $\nabla \cdot (\mathcal{N})$ yields

$$\Delta p = \mathrm{Ra} T_z$$

and taking $\Delta(\mathcal{N}_3)$ gives us

$$\Delta^2 w + \mathrm{Ra} \Delta T = \Delta p_z$$

substituting for p we form the only dynamical constraint for this problem

$$\boxed{\Delta^2 w + \mathrm{Ra} \Delta_H T = 0} \tag{4}$$

in which the horizontal Laplacian applied to T is defined as $\Delta_H = \frac{\partial^2}{\partial x^2} + \frac{\partial^2}{\partial y^2}$. So we have seen that the horizontal velocity components u, v are purely depending on the diagnostic pressure variable. In Figure (1) we show how the problem is entirely reduced to this point-wise constraint and boundary conditions for w only.

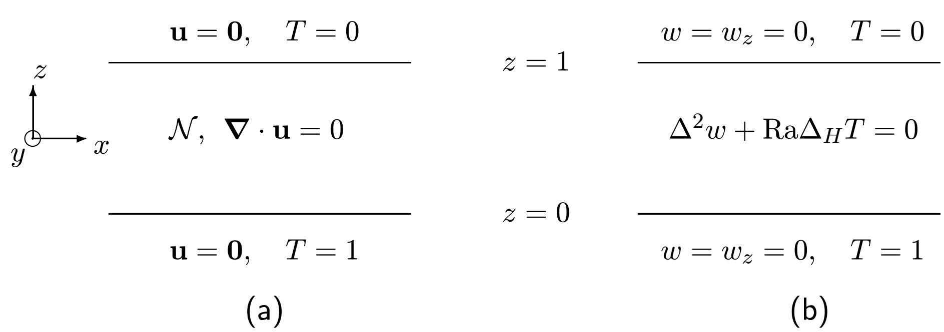

Figure 1: Comparison of the point-wise constraints and boundary conditions in (a) finite Prandtl number Rayleigh-Bénard convection and (b) infinite Prandtl number convection.

2.2 Notation

The periodic domain in x, y is defined as $[0, L_x] \times [0, L_y]$. Horizontal and global space averages can be defined:

$$\overline{(\cdot)} := \frac{1}{L_x L_y} \int_0^{L_x} \mathrm{d}x \int_0^{L_y} \mathrm{d}y \, (\cdot), \qquad \langle (\cdot) \rangle := \int_0^1 \mathrm{d}z \, \overline{(\cdot)}$$

Long-time average:

$$\langle (\cdot) \rangle_\infty = \lim_{\mathcal{T}\to\infty} \langle (\cdot) \rangle_{\mathcal{T}}$$

and the L_2-norm:

$$\|(\cdot)\| = \left\langle (\cdot)^2 \right\rangle^{1/2}.$$

For functions depending on z only we use a prime to denote the z-derivative of that function, so

$$f'(z) := \frac{\mathrm{d}f}{\mathrm{d}z}.$$

2.3 Definitions

Equation (2) can be rewritten as

$$\frac{\partial T}{\partial t} = -\boldsymbol{\nabla} \cdot (\mathbf{j} + \mathbf{J})$$

where $\mathbf{j}$ is the conductive heat flow, $\mathbf{j} := -\boldsymbol{\nabla} T$, and $\mathbf{J}$ is the convective heat flow, $\mathbf{J} := \mathbf{u}T$. In the purely conductive state the average heat transport between the plates is

$$\langle \hat{\mathbf{z}} \cdot (-\boldsymbol{\nabla} T) \rangle = -T\Big|_0^1 = 1 \tag{5}$$

The total average heat transport between the plates is

$$\langle \hat{\mathbf{z}} \cdot (\mathbf{j} + \mathbf{J}) \rangle = 1 + \langle wT \rangle \tag{6}$$

We define the Nusselt number, Nu, as the ratio of the long-time averaged total heat transport to conductive heat transport across the plates. This is simply the ratio of the expressions in Equation (6) and Equation (5), therefore we have

$$\mathrm{Nu} = 1 + \langle wT \rangle_\infty .$$

Using the global entropy flux balance, $\langle T\,\mathcal{H} \rangle = 0$,

$$\frac{\mathrm{d}}{\mathrm{d}t}\frac{1}{2}\|T\|^2 + \|\boldsymbol{\nabla} T\|^2 = 1 + \langle wT \rangle \tag{7}$$

and appealing to the temperature maximum principle, we find the following equivalent definitions of Nu as a simple consequence

$$\mathrm{Nu} = \left\langle \|\boldsymbol{\nabla} T\|^2 \right\rangle_\infty \tag{8}$$

We will see below that the point-wise constraint in Equation (4) and the global entropy flux balance constraint (7) are at the centre of both of the bounding problems.

3 Doering-Otero Approach

The background decomposition of the temperature field is

$$T(\mathbf{x}, t) = \tau(z) + \theta(\mathbf{x}, t) \tag{9}$$

where $\tau(z)$ takes up the fixed temperature boundary conditions, $\tau(0) = 1$ and $\tau(1) = 0$, and θ must therefore satisfy homogeneous boundary conditions. Substituting this change of variables into the heat equation yields

$$\frac{\partial \theta}{\partial t} + \mathbf{u} \cdot \boldsymbol{\nabla} \theta = \Delta \theta + \tau'' - w\tau'. \tag{10}$$

We have the following identity

$$\|\boldsymbol{\nabla} T\|^2 = \|\boldsymbol{\nabla} \theta\|^2 + \|\tau'\|^2 - 2\langle \theta \tau'' \rangle, \tag{11}$$

and multiplying Equation (10) by θ and taking the global average produces

$$\frac{1}{2}\frac{\mathrm{d}}{\mathrm{d}t}\|\theta\|^2 = -\|\boldsymbol{\nabla}\theta\|^2 + \left\langle \theta\tau'' - w\theta\tau' \right\rangle. \tag{12}$$

Adding $b\times$(12) to (11) gives

$$\frac{b}{2}\frac{\mathrm{d}}{\mathrm{d}t}\|\theta\| + \|\boldsymbol{\nabla} T\|^2 = \|\tau'\|^2 - \mathcal{G}(\tau, w, \theta, b) \tag{13}$$

where $\mathcal{G} = \left\langle (b-1)\|\boldsymbol{\nabla}\theta\|^2 - (b-2)\theta\tau'' + bw\theta\tau' \right\rangle$. By adding a balance parameter, b, we are generalising the work of Otero, who takes $b = 2$ to remove the centre term in $\mathcal{G}$.

Taking a long-time average we have the following upper bound on the Nusselt number

$$\boxed{\mathrm{Nu} \leq \|\tau'\|^2 - \inf \left\langle \mathcal{G}(\tau, w, \theta, b) \right\rangle_\infty} \tag{14}$$

provided that $\inf \mathcal{G}$ exists. We can drop time averages here because the infimum will be achieved by steady fields.

To minimise $\mathcal{G}$ we set up the following Lagrangian

$$L = \mathcal{G} - \langle q(\mathbf{x})(\Delta w + Ra\Delta_{_H}\theta)\rangle$$

where $q(\mathbf{x})$ is a Lagrange multiplier with natural boundary conditions which imposes the point-wise constraint in (4). By taking the horizontal average of the θ variation of L we uncover the mean of the optimal fluctuation in terms of τ

$$\frac{\delta L}{\delta \theta} = -2(b-1)\Delta\theta - (b-2)\tau'' + bw\tau' - \mathrm{Ra}\Delta_{_H} q = 0.$$

The q term drops when we take a horizontal average $\overline{\dfrac{\delta L}{\delta \theta}} = 0$, and we find that

$$2(b-1)\overline{\theta}'' + (b-2)\tau'' = 0.$$

Two integrations and consideration of the boundary conditions reveal that

$$\overline{\theta} = -\frac{(b-2)}{2(b-1)}[\tau + z - 1].$$

If we subtract off the mean part from the fluctuation field by setting $\hat{\theta} = \theta - \overline{\theta}$ and substitute this into Expression (14) we yield the following:

If $\tau(z)$ satisfies the spectral constraint $\mathcal{Q}(\tau, w, \hat{\theta}, b) = \left\{(b-1)\|\boldsymbol{\nabla}\hat{\theta}\|^2 + b\langle\hat{\theta}w\tau'\rangle\right\} \geq 0$ over all fields $(w, \hat{\theta})$ which satisfy $\Delta^2 w + \mathrm{Ra}\Delta_H \hat{\theta} = 0$ and the relavent boundary conditions (Figure 1(b)), then the following upper bound on Nu holds

$$\mathrm{Nu} - 1 \leq \frac{b^2}{4(b-1)}(\|\tau'\|^2 - 1). \tag{15}$$

We must also have $b > 1$ in order that the quadratic functional $\mathcal{Q}$ has a minimum value.

4 Howard-Chan Approach

We begin by assuming statistical stationarity for all horizontal averages, then $\langle wT \rangle_\infty = \langle wT \rangle$ and moreover

$$\mathrm{Nu} = 1 + \langle wT \rangle.$$

We make the mean-fluctuation decomposition of the temperature field $T = \overline{T} + \hat{\theta}$. Where now $\overline{T}$ is the time independent horizontal mean and $\overline{\hat{\theta}} = 0$.

A horizontal average of Equation (2) after integration gives

$$\frac{\mathrm{d}\overline{T}}{\mathrm{d}z} = \overline{w\hat{\theta}} - \langle w\hat{\theta} \rangle - 1 \tag{16}$$

and multiplying Equation (2) by T and global averaging yields

$$\left\langle \overline{T}\, \frac{\mathrm{d}^2\overline{T}}{\mathrm{d}z^2} \right\rangle = -\|\boldsymbol{\nabla}\hat{\theta}\|^2 \tag{17}$$

then inserting (16) into (17) we deduce the so-called second power integral

$$\left\| \boldsymbol{\nabla}\hat{\theta}\|^2 + \|\overline{w\hat{\theta}} - \langle w\hat{\theta}\rangle\|^2 \right\rangle = \langle w\hat{\theta} \rangle. \tag{18}$$

We can form unity by taking the ratio of terms in the previous balance

$$1 = \frac{\langle w\hat{\theta}\rangle - \|\boldsymbol{\nabla}\hat{\theta}\|^2}{\|\overline{w\hat{\theta}} - \langle w\hat{\theta}\rangle\|^2}$$

and subsequently we can define the homogeneous functional which Chan [4] seeks to maximise. Let $F := \mathrm{Nu} - 1$ and multiply the above representation of unity by $\langle w\hat{\theta}\rangle$ to form a homogeneous functional

$$\boxed{F = \frac{\langle w\hat{\theta}\rangle^2 - \langle w\hat{\theta}\rangle\|\boldsymbol{\nabla}\hat{\theta}\|^2}{\|\overline{w\hat{\theta}} - \langle w\hat{\theta}\rangle\|^2}} \tag{19}$$

the supremum of which is an upper bound on $\mathrm{Nu}-1$. The maximisation of F is performed over the competitor fields and the constraint in Equation (18) is imposed post facto by normalising $\langle w\hat{\theta}\rangle = F$.

Chan studied the following Lagrangian form

$$G = F - \langle q(\mathbf{x})(\Delta^2 w + \mathrm{Ra}\Delta_H \hat{\theta})\rangle \tag{20}$$

where q is a Lagrange multiplier satisfying natural boundary conditions which imposes the point-wise constraint in Equation (4). This is exactly the functional Eq. (25) in [4] without the normalisation $\langle w\hat{\theta}\rangle = 1$. Taking variations of this functional with respect to w and then $\hat{\theta}$ one finds that

$$\frac{\delta G}{\delta w} = \frac{\hat{\theta}(2\langle w\hat{\theta}\rangle - \|\boldsymbol{\nabla}\hat{\theta}\|^2)}{\|\overline{w\hat{\theta}} - \langle w\hat{\theta}\rangle\|^2} - \frac{2F\hat{\theta}(\overline{w\hat{\theta}} - \langle w\hat{\theta}\rangle)}{\|\overline{w\hat{\theta}} - \langle w\hat{\theta}\rangle\|^2} - \Delta^2 q = 0$$

$$\frac{\delta G}{\delta \hat{\theta}} = \frac{2\langle w\hat{\theta}\rangle(w + \Delta\hat{\theta}) - w\|\boldsymbol{\nabla}\hat{\theta}\|^2}{\|\overline{w\hat{\theta}} - \langle w\hat{\theta}\rangle\|^2} - \frac{2Fw(\overline{w\hat{\theta}} - \langle w\hat{\theta}\rangle)}{\|\overline{w\hat{\theta}} - \langle w\hat{\theta}\rangle\|^2} - \mathrm{Ra}\Delta_H q = 0$$

Multiplying these equations through by $\|\overline{w\hat{\theta}} - \langle w\hat{\theta}\rangle\|^2$ and substituting in

$$\|\boldsymbol{\nabla}\hat{\theta}\|^2 = \langle w\hat{\theta}\rangle - \|\overline{w\hat{\theta}} - \langle w\hat{\theta}\rangle\|^2$$

we deduce the following Euler-Lagrange equations for w and $\hat{\theta}$

$$\hat{\theta}\left(\langle w\hat{\theta}\rangle + \|\overline{w\hat{\theta}} - \langle w\hat{\theta}\rangle\|^2\right) - 2F\hat{\theta}\left(\overline{w\hat{\theta}} - \langle w\hat{\theta}\rangle\right) - (\Delta^2 q)\,\|\overline{w\hat{\theta}} - \langle w\hat{\theta}\rangle\|^2 = 0, \tag{21}$$

$$\begin{aligned} 2\Delta\hat{\theta}\langle w\hat{\theta}\rangle \quad &+ \quad w\left(\langle w\hat{\theta}\rangle + \|\overline{w\hat{\theta}} - \langle w\hat{\theta}\rangle\|^2\right) \\ &- \quad 2Fw\left(\overline{w\hat{\theta}} - \langle w\hat{\theta}\rangle\right) - \mathrm{Ra}(\Delta_H q)\,\left\|\overline{w\hat{\theta}} - \langle w\hat{\theta}\rangle\right\|^2 = 0. \end{aligned} \tag{22}$$

It can be shown that if we normalise w and θ as Chan does, namely $w \to \langle w\hat{\theta}\rangle^{-\frac{1}{2}} R^{-\frac{1}{2}} w$ and $\hat{\theta} \to \langle w\hat{\theta}\rangle^{-\frac{1}{2}} R^{\frac{1}{2}}\hat{\theta}$ so that $\langle w\theta\rangle \to 1$ then equations (22) and (21) become exactly the Euler-Lagrange equations (27) in [4] which Chan solves using Busse's multi-α solution.

Having derived the Doering-Otero and Howard-Chan approaches in the previous two sections we now turn to proving the duality between the two methods.

5 A Unifying Functional

Claim: The Doering-Otero principle and the Howard-Chan principle both seek to optimise the following functional

$$\boxed{N := \|\boldsymbol{\nabla} T\|^2 - b\langle\theta\,\mathcal{H}\rangle - \langle q(\mathbf{x})(\Delta^2 w + \mathrm{Ra}\Delta_{_H}\theta)\rangle} \tag{23}$$

where θ is defined as in (9) and $\mathcal{H}$ is the heat equation

$$\mathcal{H} := \frac{\partial\theta}{\partial t} + \mathbf{u}\cdot\boldsymbol{\nabla}\theta - \Delta\theta + w\tau' - \tau'' = 0$$

Proof:

We start by deriving all of the variational derivatives of N. In terms of τ and θ we have

$$\begin{aligned} N(\tau, w, \theta, b, q) = \|\tau'\|^2 - \big\langle(b-1)|\boldsymbol{\nabla}\theta|^2 - (b-2)\theta\tau'' + b\theta w\tau'\big\rangle \\ -\langle q(\mathbf{x})(\Delta^2 w + \mathrm{Ra}\Delta_{_H}\theta)\rangle \end{aligned} \tag{24}$$

Variations are taken in τ, θ, w, q and then variational equation for the mean and fluctuating part of θ are deduced.

$$\frac{\delta N}{\delta\tau} = -2\tau'' + (b-2)\overline{\theta}'' + b(\overline{w\theta})' = 0$$

$$\frac{\delta N}{\delta\theta} = 2(b-1)\Delta\theta + (b-2)\tau'' - bw\tau' - \mathrm{Ra}\Delta_{_H} q = 0$$

$$\frac{\delta N}{\delta w} = -b\theta\tau' - \Delta^2 q = 0$$

$$\frac{\delta N}{\delta q} = \Delta^2 w + \mathrm{Ra}\Delta_{_H}\theta = 0$$

$$\frac{\delta N}{\delta\theta} = 0 \qquad \left\{ \begin{aligned} \frac{\delta N}{\delta\overline{\theta}} &= 2(b-1)\overline{\theta}'' + (b-2)\tau'' = 0 \\ \frac{\delta N}{\delta\hat{\theta}} &= 2(b-1)\Delta\hat{\theta} - bw\tau' - \mathrm{Ra}\Delta_{_H} q = 0 \end{aligned} \right\}$$

Part 1: <u>**Doering-Otero Principle**</u>

Solve $\dfrac{\delta N}{\delta\overline{\theta}} = 0$.

Two integrations give

$$\overline{\theta} = \frac{b-2}{2(b-1)}\left[\tau + z - 1\right]$$

Plugging this into N we have

$$N(\tau, w, \hat{\theta}, b, q) - 1 = \frac{b^2}{4(b-1)}\left(\|\tau'\|^2 - 1\right) - \left\langle (b-1)|\boldsymbol{\nabla}\hat{\theta}|^2 + b\hat{\theta}w\tau' \right\rangle - \langle q(\mathbf{x})(\Delta^2 w + \mathrm{Ra}\Delta_H \hat{\theta})\rangle$$

Compare this with the functional Otero studies. Setting $b = 2$ we have $N = \|\tau'\|^2 - \left\langle |\boldsymbol{\nabla}\hat{\theta}|^2 + 2\hat{\theta}w\tau' \right\rangle - \langle q(\mathbf{x})(\Delta^2 w + \mathrm{Ra}\Delta_H \hat{\theta})\rangle$ and the fluctuation field has no mean part. It is clear that we must require $b > 1$ to ensure that a minimum of the right hand side exists.

Part 2: Howard-Chan Principle

Solve $\dfrac{\delta N}{\delta \overline{\theta}} = 0$ and $\dfrac{\delta N}{\delta \tau} = 0$ simultaneously to deduce equations for the background field and the mean of the fluctuation field in terms of the mean-less fluctuation field $\hat{\theta}$.

$$\left\{\begin{array}{l} \tau' = \dfrac{2(b-1)}{b}\left\{\overline{w\theta} - \langle w\theta\rangle\right\} - 1 \\[2ex] \overline{\theta}' = -\dfrac{b-2}{b}\left\{\overline{w\theta} - \langle w\theta\rangle\right\} \end{array}\right\}$$

Plug these expressions into N, of Equation (24), noticing that $\overline{w\theta} = \overline{w\hat{\theta}}$, after some algebra we have

$$N(w, \hat{\theta}, b, q) = 1 + \langle w\hat{\theta}\rangle + (b-1)\left\{\langle w\hat{\theta}\rangle - \|\overline{w\hat{\theta}} - \langle w\hat{\theta}\rangle\|^2 - \|\boldsymbol{\nabla}\hat{\theta}\|^2\right\} - \langle q(\mathbf{x})(\Delta^2 w + \mathrm{Ra}\Delta_H \hat{\theta})\rangle \quad (25)$$

Now we see that the Lagrange multiplier b is imposing the global entropy flux balance (Equation 18) and q is imposing the point-wise constraint in Equation (4). The remaining variational equations for w and $\hat{\theta}$ are

$$\frac{\delta N}{\delta \hat{\theta}} = w + (b-1)\left\{w - 2w\left(\overline{w\hat{\theta}} - \langle w\hat{\theta}\rangle\right) + 2\Delta\hat{\theta}\right\} - \mathrm{Ra}\Delta_H q = 0 \quad (26)$$

$$\frac{\delta N}{\delta w} = \hat{\theta} + (b-1)\left\{\hat{\theta} - 2\hat{\theta}\left(\overline{w\hat{\theta}} - \langle w\hat{\theta}\rangle\right)\right\} - \Delta^2 q = 0 \quad (27)$$

We can calculate $\langle \hat{\theta}\,\dfrac{\delta N}{\delta \hat{\theta}}\rangle = 0$ and $\langle w\,\dfrac{\delta N}{\delta w}\rangle = 0$ in order to obtain a value for b. The equations to be solved are

$$(2-b)\langle w\hat{\theta}\rangle - \mathrm{Ra}\langle (\Delta_H q)\hat{\theta}\rangle = 0$$

and

$$(2-b)\langle w\hat{\theta}\rangle + 2(b-1)\|\nabla\hat{\theta}\|^2 - \langle(\Delta^2 q)w\rangle = 0.$$

Given that $\langle(\Delta^2 q)w\rangle = \langle q(\Delta^2 w)\rangle = \langle q(-\mathrm{Ra}\Delta_H \hat{\theta}\rangle$ we can add these two equations and solve for b to find that

$$\boxed{b = \frac{\|\nabla\hat{\theta}\|^2 - 2\langle w\hat{\theta}\rangle}{\|\nabla\hat{\theta}\|^2 - \langle w\hat{\theta}\rangle}} \tag{28}$$

With the use of the second power integral we can rearrange this expression to give

$$b - 1 = \frac{\langle w\hat{\theta}\rangle}{\|\overline{w\hat{\theta}} - \langle w\hat{\theta}\rangle\|^2} \tag{29}$$

for easy insertion back into Equations (26) and (27). Inserting and multiplying the resulting expressions through by $\|\overline{w\hat{\theta}} - \langle w\hat{\theta}\rangle\|^2$ we arrive at the expressions

$$\hat{\theta}\left(\langle w\hat{\theta}\rangle + \|\overline{w\hat{\theta}} - \langle w\hat{\theta}\rangle\|^2\right) - 2\hat{\theta}\langle w\hat{\theta}\rangle\left(\overline{w\hat{\theta}} - \langle w\hat{\theta}\rangle\right) - (\Delta^2 q)\,\|\overline{w\hat{\theta}} - \langle w\hat{\theta}\rangle\|^2 = 0 \tag{30}$$

$$\begin{aligned} 2\Delta\hat{\theta}\langle w\hat{\theta}\rangle + w\left(\langle w\hat{\theta}\rangle + \|\overline{w\hat{\theta}} - \langle w\hat{\theta}\rangle\|^2\right) - 2w\langle w\hat{\theta}\rangle\left(\overline{w\hat{\theta}} - \langle w\hat{\theta}\rangle\right) \\ -\mathrm{Ra}(\Delta_H q)\,\|\overline{w\hat{\theta}} - \langle w\hat{\theta}\rangle\|^2 = 0 \end{aligned} \tag{31}$$

Replacing the $\langle w\hat{\theta}\rangle$ which multiply $\left(\overline{w\hat{\theta}} - \langle w\hat{\theta}\rangle\right)$ in both equations by the functional F we have exactly the Euler-Lagrange equations that were derived from Chan's homogeneous ratio (Equations 21-22).

As a final comment we note that for the problems to intersect the Howard-Chan problem must also satisfy the spectral constraint so that the top maximum is selected. This means that $(b-1) > 0$, which is consistent with Equation (29) since $\langle w\hat{\theta}\rangle$ is positive due to the second power integral.

6 Piecewise Linear Background Profiles

In the framework of the Background method rigorous upper bounds on Nu are easily calculated by using piecewise linear test profiles for τ (see Figure 2). These functions are odd functions about the channel midplane, they take the value of 1/2 in the interior of the channel and change linearly over two boundary layers of thickness δ, such that they satisfy the boundary conditions on τ, and the derivative of τ is:

$$\tau' = \left\{ \begin{array}{ll} 0 & \text{for } z \in (\delta, 1-\delta) \\ \frac{1}{2\delta} & \text{otherwise.} \end{array} \right\}$$

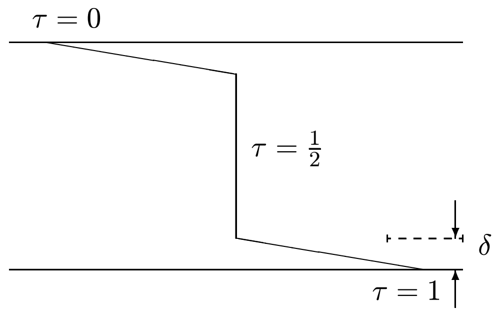

Figure 2: Piecewise linear τ.

We take $b = 2$ in keeping with Otero [9], in which case $Nu \le \langle \tau'^2 \rangle$. Simple integration shows that the upper bound on the heat transport is $Nu \le \dfrac{1}{2\delta}$ if τ satisfies the following condition

$$\boxed{\tau \text{ is an admissible test function if } \inf Q \ge 0} \tag{32}$$

for all $w$and θ with $\Delta^2 w + Ra\Delta_H \theta = 0$ and $w = Dw = \theta = 0$ at $z = 0, 1$.

The piecewise linear profile which produces the lowest upper bound is found by minimising the following functional

$$\mathcal{G} = Q - \langle q(\mathbf{x})(\Delta w + Ra\Delta_H \theta)\rangle + 2\lambda(\langle \theta^2 \rangle - 1)$$

where q is a point-wise Lagrange Multiplier imposing the momentum constraint, and λ is used to normalise θ. The Euler-Lagrange equations for this functional are

$$\lambda\theta = (D^2 - k^2)\theta - w\tau' + \frac{Ra}{2}k^2 q, \tag{33}$$

$$0 = 2\theta\tau' + (D^2 - k^2)^2 q, \tag{34}$$

$$0 = (D^2 - k^2)^2 w - Rak^2\theta, \tag{35}$$

where all of the fields have been Fourier expanded as $f = f(z)e^{ikx}$, and each variable q, w, and θ now only depend on z and must satisfy the following boundary conditions

$$\theta = w = Dw = q = Dq = 0 \qquad \text{at } \ z = 0, 1.$$

Given that only τ' is discontinuous at $z = \delta$ and $z = 1 - \delta$ we must solve for w, θ and q inside three regions $[0, \delta]$, $[\delta, 1 - \delta]$ and $[1 - \delta, \delta]$, and impose matching conditions between the regions. Since equations (33-35) are second order in θ and fourth order in w and g, the natural matching conditions are

$$[\theta] = [D\theta] = 0$$

$$[D^i w] = [D^i g] = 0 \qquad \text{for } \ i = 0, 1, 2, 3$$

where $[f]$ denotes the jump in the value of f at either $z = \delta$ or $z = 1 - \delta$, and the superscript denotes the nth z-derivative.

6.1 Solution Using Complex Eigenfunctions

In Otero's thesis he successfully applies the method of finding complex analytic eigenfunctions to many variational problems in turbulent convection. The assumption is made, and later accounted for, that the most critical eigenfunctions are even about the mid-plane. Thus the following symmetry conditions are also imposed:

$$D\theta = Dw = D^3w = Dg = D^3g = 0 \qquad \text{at } \ z = 1/2.$$

The solutions is then required in only two regions:

$$\text{Region I: } [0, \delta] \quad \text{Region 2: } [\delta, 1/2].$$

λ is set to zero and equations (33- 35) are solved in complex eigenfunctions on each region. The boundary conditions at $z = 0$ are built in to the solution in Region I and the symmetry conditions at $z = \frac{1}{2}$ are built in to the solution in Region II. The 10 matching condition are used to specify 10 unknown coefficients in the two solutions. These conditions can be collected in to a 10×10 linear homogeneous system, say $Mx = 0$, where x represents a vector of 10 unknown coefficients. Non-trivial solutions exist if $\det M = 0$. The following numerical recipe is used to optimise the upper bound:

Technique:

- Fix Ra.
- For fixed k graph $\det M$ versus δ and find the minimum δ such that $\det M = 0$, label this δ_0.
- Select the minimum δ_0 over all k, label this δ_c.

Then δ_c corresponds to the largest δ for which condition(32) holds and hence the lowest upper bound for piecewise linear profiles is $Nu \leq \dfrac{1}{2\delta_c}$.

6.2 Calculating the Eigenvalue Spectrum of Constraint (32)

It is easily shown by multiplying Equation (33) by θ, globally averaging and using constraints (34) and (35), that $Q = -\lambda$. Condition (32) is thus equivalent to requiring that the highest eigenvalue, say λ_0, of eigenvalue problem (33) subject to (34) and (35), over all k-space are negative semi-definite. We can therefore repose condition(32) as

$$\boxed{\begin{array}{c}\tau \text{ is an admissible test function if} \\ \lambda_0^* := \max_k \lambda_0 \ \text{ satisfies } \ \lambda_0^* \leq 0.\end{array}} \tag{36}$$

We calculate the spectrum $\lambda_0(k)$ of Equations (33-35) using finite difference methods together with the shooting technique to match the solutions on each region at the point $z = \delta$. λ_0^* is found to be a monotone increasing function of δ. We are able to find the critical δ, say δ_c, for which $\lambda_0^* = 0$ as illustrated below.

Technique:

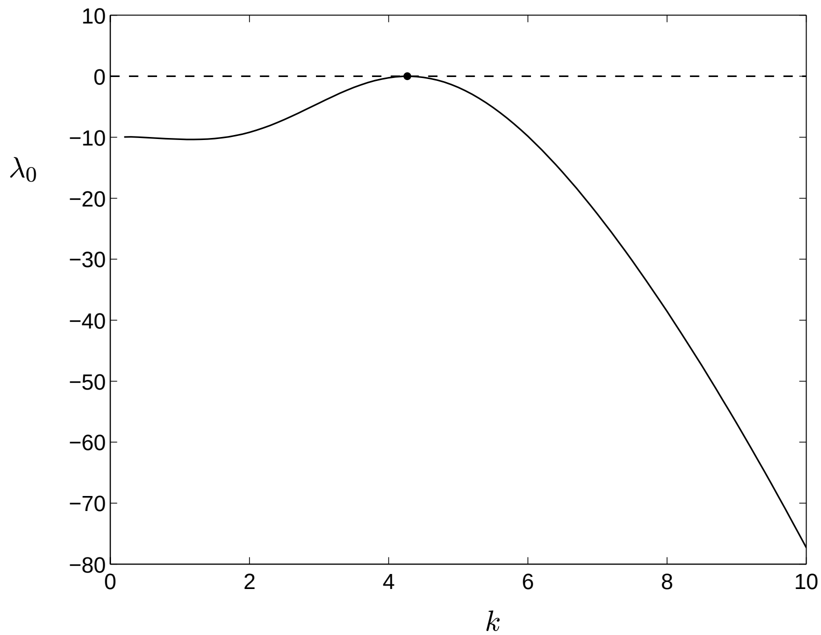

Figure 3: The spectrum of Equations (33-35) at $Ra = 10^9$ and optimal boundary thickness $\delta_c = 1.3457 \times 10^{-3}$.

- Fix Ra.
- For fixed δ calculate $\lambda_0(k)$ and find its maximum λ_0^*
- Vary δ until $\lambda_0^* = 0$

The envelope of the eigenvalue spectrum $\lambda_0(k)$ is found to have a unique maximum. We denote the wavenumber at which the maximum occurs by k_c. This procedure leads us to the critical δ for which condition (36) is marginally satisfied. It is the same δ as calculated by the numerical scheme used by Otero. Figure 3 shows an example of the spectrum at $Ra = 10^9$.

6.3 Comparison of Numerics

For comparison of our numerical technique with that of Otero we calculate δ_c at six points in $\log(Ra)$-space between 4 and 9. The results are shown in Figure 5. The solid upper line is plotted using data supplied by Otero. Our calculation is shown as circles which fall reassuringly well on top of Otero's data. Also shown is Chan's optimal upper bound with a 1/3 scaling taken directly from his 1971 publication. Also of interest here are the crosses which are associated to a lower bound on the optimal upper bound calculated here to explore the nature of the duality which exists between the Howard-Chan method and the Doering-Otero method. We took the eigenfunctions for w and θ associated with the critical

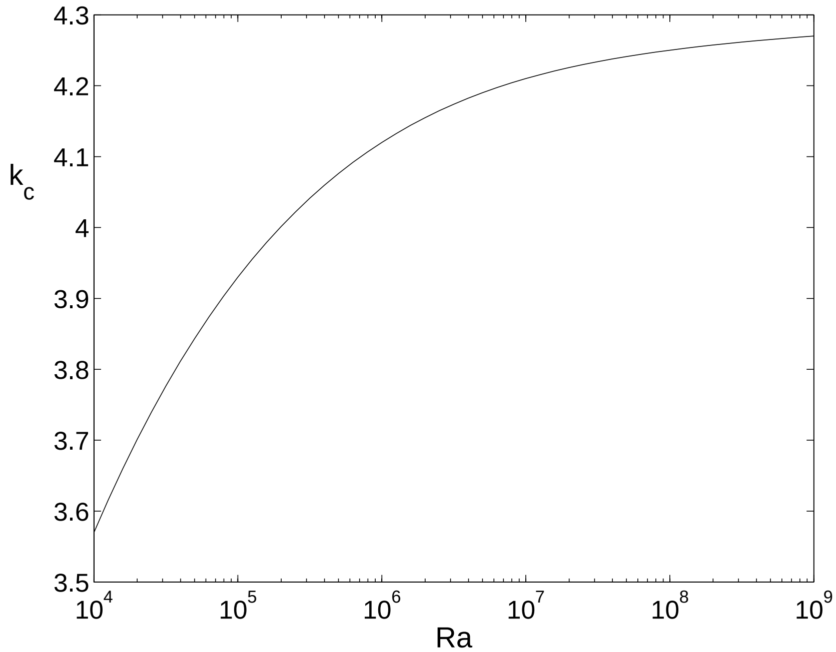

Figure 4: The critical wavenumber for the optimising piecewise linear profiles. This shows that $k_c \sim O(1)$.

wavenumber k_c when $\lambda_0^* = 0$ and evaluated Chan's homogeneous functional (19) at these points. This procedure guarantees a lower bound on Chan's optimal upper bound. However, this lower bound is very poor and this naive experiment reveals that the eigenfunctions (see Figure 7) do not well approximate the structure of Chan's optimal solutions (see Figure 6) and are thus poor test functions for the Howard-Chan variational problem. One notices, for example, that there is no boundary layer in the product $w\theta$ for our eigenfunctions.

Interestingly the critical wavenumber of the optimal piecewise linear profile remains order one for all Ra studied here (see Figure 4).

7 Discussion

To summarise we have confirmed Otero's numerical calculation and we have shown that the duality shared between the two variational problems discussed here is worth further investigation.

In all other cases, for example plane Couette flow, pipe flow and arbitrary Prandtl number convection, where piecewise linear test profiles have been applied within the Background method the correct optimal scaling of the upper bound was achieved. In this case Chan's result presents $1/3$ as the optimal scaling of Nu with Ra however the piecewise linear profiles are capturing $2/5$ instead. We note briefly that we have solved this problem without setting $b = 2$ and have found that optimising the upper bound over the balance parameter b does not alter the $2/5$ scaling of this upper bound result.

To conclude we would like to propose that future work on this problem should be

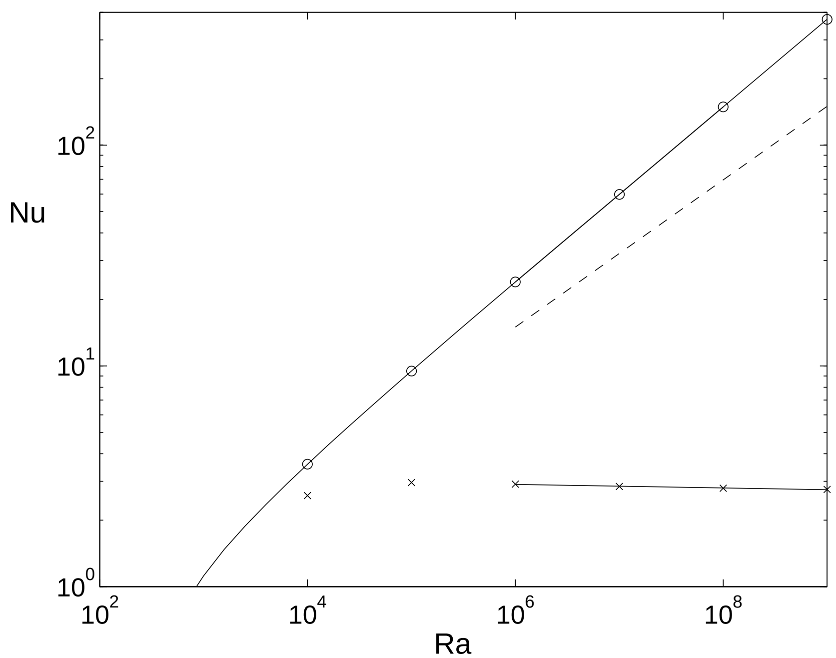

Figure 5: The numerical upper bound for the Background method with piecewise linear profile. The upper solid line is the upper bound calculated by Otero. Circles are the points calculated during this study. The dashed line is Chan's multi-α upper bound. The crosses are a lower bound on the optimal bound which was calculated by evaluating Chan's functional with the eigenfunctions associated to the critical wavenumbers.

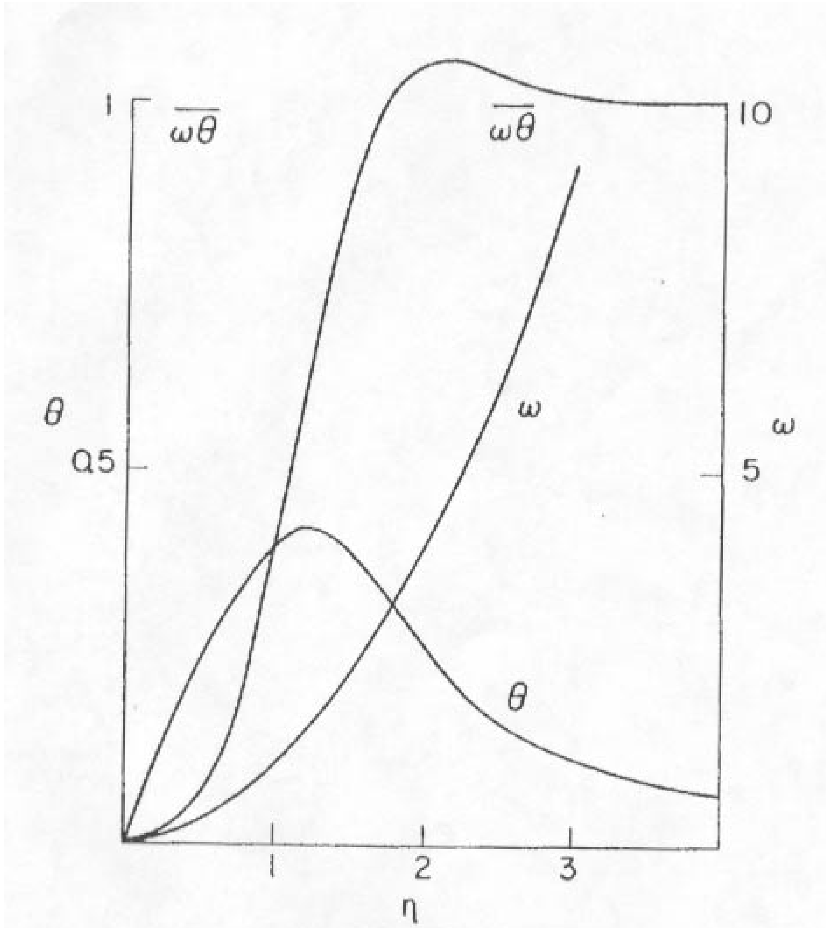

Figure 6: The z-structure of Chan's optimal solutions.

concerned with solving the full optimal Background problem, as done recently in [10] for the problem of plane Couette flow, or as an intermediate step, to study how more sophisticated test profiles, such as profiles with non-zero internal gradients, can improve the upper bound.

This work has been completed with the help of C. Doering, L. Howard, G. Ierley, R. Kerswell and J. Otero. I thank all of them for their insightful advice and their enthusiasm for this problem. I would also like to thank all of the students and staff of the Woods Hole program who together made the Summer an unforgettable experience. Finally I hope that the legendary GFD Dynamos softball team have many more triumphant years to come under the auspices of George Veronis.

References

[1] L. N. Howard, "Heat transport by turbulent convection," J. Fluid Mech. **17**, 405 (1963).

[2] L. N. Howard, "Bounds on flow quantities," Annu. Rev. Fluid Mech. **4**, 473 (1972).

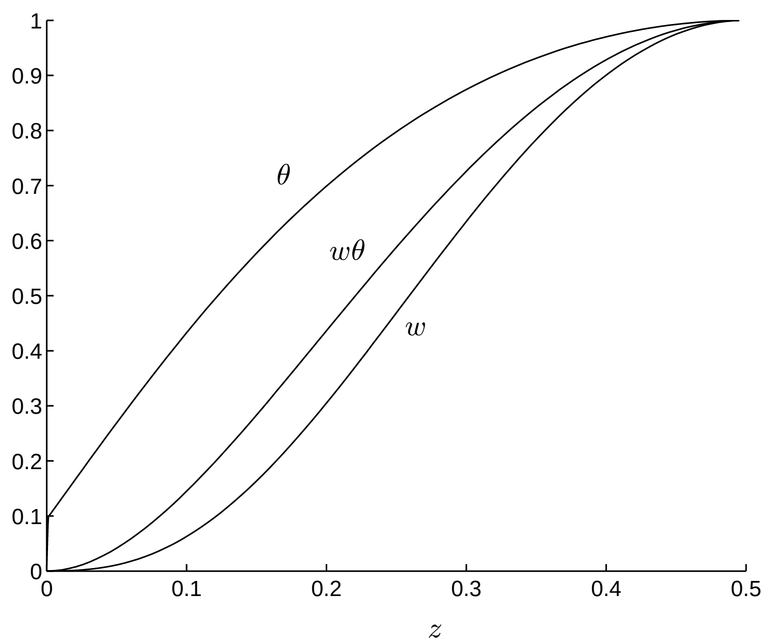

Figure 7: The normalised z-structure of the eigenfunctions associated with the critical wavenumber in the piecewise linear optimal upper bound.

[3] F. H. Busse, "On Howard's upper bound for heat transport by turbulent convection," J. Fluid Mech. **37**, 457 (1969).

[4] S.-K. Chan, "Infinite Prandtl Number Turbulent Convection," Stud. Appl. Math. **50**, 13 (1971).

[5] C. R. Doering and P. Constantin, "Variational bounds on energy dissipation in incompressible flows. III. Convection," Phys. Rev. E **53**, 5957 (1996).

[6] R. R. Kerswell, "New results in the variational approach to turbulent Boussinesq convection," Phys. Fluids **13**, 192 (2001).

[7] C. R.Doering and P. Constantin, "On upper bounds for infinite Prandtl number convection with or without rotation," J. Math. Phys. **42**, 784 (2001).

[8] P. Constantin and C. R. Doering, "Infinite Prandtl number convection," J. Statist. Phys. **94**, 159 (1999).

[9] J. Otero, Ph.D. thesis, University of Michigan, 2002.

[10] S. C. Plasting and R. R. Kerswell, in press (unpublished).